

# Temperature Effect on the Operation of Elementary Quantum-Dot Spin Gates by the Example of the NOT-AND Gate

Alexey V. Krasheninnikov and Roman A. Koltsov

Moscow State Engineering Physics Institute (Technical University),  
Moscow, 115409, Russia

The effect of temperature on the operation of the elementary quantum-dot spin gates for single-electron computing is studied theoretically within the framework of the Hubbard model by the example of the NOT-AND gate. The calculated values of the uniform external magnetic field necessary to realize the whole truth table proved to be unreasonably high for the implementation of the NOT-AND logical function even at the liquid helium temperature. This result appears to be common to all spin gates. Thus, finite temperatures seem to be a serious obstacle for the practical realization of ground state calculations in quantum-dot spin gates.

## 1. Introduction

The problem of miniaturization of electronic computer components attracts much attention nowadays. The Si-based MOSFET technology is expected to enter a critical period in the beginning of the next millennium, since the minimum feature size of the computer basic unit, the transistor, will be about 0.1 micron that time if the empirical trend called as "Moore Law" [1] will remain correct in the near future. Further reduction in size seems to be inefficient [2]. Indeed, if even technological problems such as uncontrolled variation in transistor characteristics from specimen to specimen due to nonuniform distribution of doping atoms, Joule resistance heating, electromigration of atoms resulting from the extremely high current densities, etc. will be circumvented, there appear the fundamental limitations on the transistor operation related with the laws of quantum mechanics. Obviously, the classical picture is not correct on the nanometer scale, and a device must function based on quantum effects such as energy quantization and tunneling rather than in spite of them [3]. Thus, the future of computing is closely related with the development of intrinsically quantum nanometer-scale replacements for the bulk-effect semiconductor transistors.

Although the operating principles of even individual quantum devices and the interconnection problem are challenging tasks for scientists, advantages of nanocomputers such as high operation speed and low power consumption have been an enormous stimulus for the development of various approaches to the computations on the nanoscale.

Among them the theory of quantum computation is an extremely exciting and rapidly growing field of investigation [4]. This concept originating from the early works of Richard Feynman [5] and David Deutsch [6] in 1980s is based on the superposition, interference, entanglement and other fundamental properties [7] of a quantum system. Quantum computer requires quantum logic: it deals with the quantum bits or qubits, for short, i.e. with an arbitrary superposition of pure classical bits, 0 and 1. Unlike its classical counterpart, quantum computers use "quantumness" at the information-theoretical level. Quantum computations are reversible, and all states in the superposition of qubits are processed simultaneously, so the calculation may be speeded up exponentially [8]. The Shor's [9] discovery of quantum algorithms for the integer factorization and for the discrete logarithm, that run exponentially faster [10] than the best known classical algorithms and the experimental demonstrations [11], [12] of a single elementary unit of a quantum computer gave rise to a dramatic growth in the number of publications on quantum computations. At the same time, practical implementation of a quantum computer and, in general, feasibility of quantum computations in a physical system casts serious doubts [8], [13], [14]. The principal issue is the ratio of quantum computation speed to the decoherence rate [15]. There are fundamental limitations [8] related to the particular implementation of a quantum computer (e.g., a rate at which lasers may drive atomic transitions of a given lifetime, etc.) that inevitably decrease computational speed. So the decoherence, inherent for any real physical system, is believed never to be reduced to the point where more than a few consecutive quantum computational steps can be made [13].

Other approaches such as mechanical [16], chemical [17], [18] and electronic nanocomputing [19], [21], [20] employ classical Boolean logic. Upon development of these concepts many aspects of conventional computation realized in semiconductor microcomputers are taken into account. (Recall that quantum computational algorithms are shown to be more efficient than classical ones for the two problems only [9], [10]). But the basic units of nanocomputers differ fundamentally from usual microtransistors, being about several nanometers in size.

The theoretical possibility for building mechanical nanocomputers was demonstrated in [16, 22]. Such computers, if constructed, would operate like a vastly scaling down program mable version of the mechanical calculators appeared in

the 1940s. The data processing is performed with the help of moving molecular-scale rods and rotating molecular-scale wheels assembled by the mechanical positioning of atoms and molecules using STM. The fabrication of such devices is tedious task demanding the perfection and development of STM-technology. Besides, other practical issues must be addressed, such as how to power and program nanomachinery [3].

The operation of a chemical nanocomputer is based on the storage of data in chemical (i.e. molecular) structures. Information processing is performed by making and breaking chemical bonds. The existing biochemical variants of such computers are humans and animals nervous systems. Unfortunately, the artificial fabrication of this category of nanocomputers seems to be far beyond the experimental realization, since the mechanisms for animal brains and nervous systems are poorly understood. Nevertheless, a complex graph theory problem has been solved recently on sequences of DNA's molecular subunits [17]. This approach being a giant leap towards the creation of a biochemical computer may be applied not only to the solution of combinatorial problems, but to a much wider class of digital computations [18]. Note that despite a number of remaining obstacles such as efficient input and output, error correction etc., only this type of nanocomputers among mentioned above is demonstrated for an actual calculation.

The information processing in electronic nanocomputers is related with the storage and movement of electrons. There exist various propositions to use a quantum mechanical nanosystem for calculations in such a way.

For example, Lent et al. [19] suggested constructing a two-state cell made of five quantum dots having two electrons. These electrons can exist inside the cell in two equally probable states, so the polarization of a cell represents a binary zero or one. The polarization of an individual cell may be fixed by applying an appropriate voltage on an external probe or due to effect of another cell. Rows of closely arranged quantum dot cells can carry signals (i.e. change polarization), or realize various logical functions (e.g. NOT, AND, OR etc.).

Korotkov et al. [20] proposed for computing wire-like structures composed of quantum dots placed in a global electric field. Each localelement is a row of quantum dots. A neighboring element is a similar row of quantum dots perpendicular to the first. A signal is propagated through the system by the formation of electron-hole pairs in each row of quantum dots. The electric field allows the local polarization of the electron-hole pair in one element which in turn induces the formation and polarization of a pair in the next element. Thus, chains of elements could be linked together to implement elementary logical functions.

The concept of computing by measuring spins of individual electrons on quantum dots was originally introduced by Bandyopadhyay et al. [21]. In the context of this approach a computer is supposed to consist of spatially arranged arrays of tunnel-coupled quantum dots on a substrate. Each dot has single size-quantized energy level. The total number of electrons in the system, controlled by adjusting the voltage of substrate [23] is approximately equal to the number of dots, thus there is one electron per dot on the average. Bits of information are spins of individual electrons on a given quantum dot, e.g. the "up" ("down") direction of electron spin corresponds to the logical 1 (0). The temperature of the system is supposed to be equal to zero. The information is stored in the spin configuration of the system, i.e. it is conditioned by a set of quantum-mechanical ground state average values of the spin projection operator  $\hat{S}_{zi}$  on the  $i$ -th dot in the array.

Although it is not obvious a priori, it is believed that operation of the whole "spin computer" may be described considering operation of separated spin gates, by analogy with today's computers. "Gate" is an elementary unit of a computer capable to perform simplest logical functions. The example of spin gates is the "NOT-AND" gate, see Fig.1. Each gate has input and output dots. The number of such dots in the gate depends on its logical function. "NOT-AND" gate has two input (A, B) and one output dot (Y). The former serve for writing the input signals to the gate by the action of an external agent (e.g. local magnetic field generated by a magnetic tip of STM). As a result of external influence on input dots, the new ground state of the system is different from the initial one, so the spin configuration represents the result of a desired computational operation. Upon such a process the electron tunneling between adjacent dots and Coulomb repulsion of electrons provide the propagation of the "signal" from dot to dot. The result of calculation may be read off from output dots by means of, e.g., magnetic tip since the tunneling current depends on the mutual orientation of the magnetizations of the dot and tip. The correspondence between magnetizations of output and input dots is uniquely determined by the logical truth table of a particular gate. The logical truth table of NOT-AND gate is shown in Fig.1.

The operation of spin gates was studied theoretically in [24], within the spin-1/2 Heisenberg model by means of the exact diagonalization technique. It was shown that for a number of the simplest logical gates, such as NOT, AND, NAND, OR, NOR, NXOR and half-adder, the entire truth table can be obtained by the appropriate choice of values of the local magnetic fields on the input dots. Since the logical variables 0 and 1 were associated with ground state averages of the spin projection operator  $\hat{S}_{zi}$  on  $i$ -th quantum dot, the threshold value  $S_t$ , ( $0 < S_t < 1$ ) of the projection of electron spin on the  $z$  axis was introduced [24]. The case  $\langle \hat{S}_{zi} \rangle = S_t = 2$  was supposed to correspond to logical one, and  $\langle \hat{S}_{zi} \rangle = S_t = 0$  to logical zero. It should be noted that in [24] this threshold value was chosen to be sufficiently low, usually  $S_t = 0.05 \dots 0.1$  (The entire truth table could not be realized otherwise). Such small values

of  $S_z$  result in a high probability of error upon measurement (this problem is discussed at length in [28]) due to a quantum-mechanical nature of electron spin. The arising necessity of "redundancy", i.e. the need for repeating the calculation process several times or for additional logic gates that work simultaneously will have deleterious effect on the operation of "spin computers". Besides, the physical truth tables, calculated in [24] were not symmetrical with respect to the input signal. E.g., the 011 and 101 rows of the logical truth table of the NOT-AND gate are never realized at equal absolute values of local magnetic fields on the gate input dots [25].

A new approach to the implementation of certain logical functions in spin gates was proposed in [25]. It was shown that placing a gate in a uniform external magnetic field  $H_z$  allows one to remove the lack of symmetry of the physical truth table and enlarge the absolute magnitudes of the average spins at the output dots. It also was demonstrated [26] that the introduction of "ferromagnetic chains" into the gate structure and application of local constant magnetic fields acting on particular dots can substantially improve the physical truth table of gates. Thus, with the elimination of the "small spin problem" the incorporation of gates into a large circuit may be possible.

Unfortunately, the operation of a spin gate computer has other fundamental limitations. One of them is related with the ground state computing concept itself. This concept underlies not only spin gates computers, but many other semiconductor quantum-dots-based logic devices [29]. Since the computation is related with the relaxation of the system into a new ground state under the influence of the external source, the speed of the operation is determined by the dissipative coupling between the system and the environment. The rate, at which the dissipation in bulk semiconductors occurs, is conditioned predominantly by the emission of a longitudinal optical phonon. This rate is equal to  $10^{12} \text{ s}^{-1}$ . At the same time, such a process is prohibited in quantum dots because of the discrete nature of the energy spectrum, unless the level separation equals to the longitudinal optical phonon energy. As was shown in [29], the longitudinal-acoustic phonon emission is the main contributor to the relaxation process in quantum dots, since the acoustic phonons have continuous spectra from zero up to a certain limiting energy. The relaxation rate was predicted to be  $(10^6 - 10^9) \text{ s}^{-1}$  [29]. Obviously, such an operation speed is too low for consideration of semiconductor spin gates as contenders for a new generation of logic devices. Note, however, that other relaxation mechanisms (e.g. interface-phonon scattering) are possible giving rise to the increase in the device functioning speed.

But even if the above limitations will be circumvented, there remains the negative effect of finite temperatures on the operation of a real spin gate computer.

If the temperature  $T \neq 0$ , quantum-mechanical ground state average values of spin projection operators must be replaced with the thermodynamical averages. It is clear a priori, that the temperature will decrease the values of  $\hat{S}_{zi}$ , resulting in the enhancement of the error probability and in the "shrinkage" of the physical truth table. But one may hope that increasing the external stabilizing field may provide the operation of spin gates at the temperatures that may be achieved in the reality, e.g. the liquid nitrogen temperature, or at least, helium temperature. It is the purpose of the paper to elucidate this issue and to establish the quantitative relations between the temperature and other parameters of the system, at which logic gates could be working.

## 2. Theoretical Model for the Spin Gates

Provided that each dot has a single size-quantized level, interacting electrons on dots may be described by a suitably parametrized Hubbard model [30] taking into account the tunneling and the intradot Coulomb repulsion of electrons. We do not consider the interaction of electrons occupying different dots, since its energy is much smaller than the intradot repulsion (see also [28]). The relevant Hamiltonian has the form:

$$H = \sum_{\langle ij \rangle} t (a_i^\dagger a_j + H.c.) + \sum_i n_i H_i \text{sign} + U \sum_i n_i n_{i\#}; \quad (1)$$

where  $a_i$  ( $a_i^\dagger$ ) is the operator of annihilation (creation) of electron on the  $i$ -th dot with spin projection  $\sigma = +1$  or  $-1$  on the  $z$ -axis,  $n_i = a_i^\dagger a_i$  is the electron number operator,  $t$  is the matrix element for hopping of electrons between quantum dots,  $U$  is the intradot Coulomb repulsion energy,  $H_i$  is the local magnetic field (along  $z$ -axis) at the  $i$ -th dot,  $\sum_B$  is the Bohr magneton,  $\langle ij \rangle$  means the summation over nearest the neighbor dots. In what follows, we set  $\sum_B = 1$ .

It is supposed that the total number of electrons  $N = \sum_i n_i$  coincides with the number of dots in the gate and the ratio  $U/t$  is large enough to provide strong antiferromagnetic correlations in the gate. These correlations result in the switching of electron spins in the gate after the local fields  $H_i$  have acted on the input dots.

In order to determine the physical truth table, i.e. the range of control signals (local magnetic fields at the input dots) for which the logical truth table of a particular gate is realized, it is necessary to calculate the ground state wave function of the Hamiltonian (1) if  $T = 0$  and in general case all the wave functions if  $T \neq 0$ . For the relatively small number of dots in the gate this can be done numerically by an exact diagonalization method [31]. At

temperatures the quantum mechanical ground state average value of spin projection operator  $\hat{S}_{zi}$  on the  $i$ -th dot in the array is determined by the well-known formula

$$\langle \hat{S}_{zi} \rangle = \frac{\sum_k \langle \hat{S}_{zi} \rangle \exp(-\beta E_k) \langle \psi_k |}{\sum_k \exp(-\beta E_k) \langle \psi_k |} \quad (2)$$

where  $\langle \psi_k |$ ;  $k = 0; 1; 2; \dots$  is the  $k$ -th eigen function of the Hamiltonian (1).

### 3. Constructing the Physical Truth Table

The procedure of the physical truth table construction may be illustrated by the example of the NOT-AND gate. Suppose that  $T = 0$ . Having the ground state wave function obtained, one can determine the resulting values of electron spin on input ( $\langle \hat{S}_{Ai} \rangle$ ,  $\langle \hat{S}_{Bi} \rangle$ ) and output ( $\langle \hat{S}_{Yi} \rangle$ ) dots after the local fields have acted. If, e.g.,  $\langle \hat{S}_{Ai} \rangle > S_t = 2$ ,  $\langle \hat{S}_{Bi} \rangle > S_t = 2$ , and  $\langle \hat{S}_{Yi} \rangle < S_t = 2$  at given values of  $H_A$  and  $H_B$ , then the first row (110) [ABY] of the logical truth table of the NOT-AND gate is realized, and we mark the point ( $H_A; H_B$ ) in the  $H_A - H_B$  plane by the symbol "+" (see Fig.2). If the spin configuration corresponds to one of the other three rows of the logical truth table (011, 101, or 001), then the point ( $H_A; H_B$ ) is marked by other symbol (since the domains are well spatially separated for the NOT-AND gate we marked all the domains by the same symbol). The blank space in the  $H_A - H_B$  plane means that none of the rows of the logical truth table is realized at given values of  $H_A$  and  $H_B$ . The procedure is absolutely the same if  $T \neq 0$ .

### 4. Results of Calculations and Discussion

The calculated physical truth tables of the NOT-AND gate at various temperatures are shown in Fig.3 for  $S_t = 0.5$ . We deliberately chose the value of  $S_t$  being not very large. Although the decrease in  $S_t$  gives rise to the enhancement in the probability to read out the incorrect result of calculation, it is instructive to show the effect of temperature on the physical truth table for such values of  $S_t$  when the range of temperatures at which the gate still works is not too small (the quantitative relation between the threshold values of  $S_t$  and maximal operating temperature will be established below).

The parameters of Hamiltonian (1) and regions of the input signals  $H_A$  and  $H_B$  are the same as in [25]:  $U = t = 20$ ;  $H_z = t = 0.05$ . Notice that the ratio  $U = t$  is large enough to provide the antiferromagnetic correlations in the system. The value of a uniform external magnetic field  $H_z$  is close to the optimum one, i.e. to the field at which the projection of electron spin on the output dot on the  $z$  axis reaches its maximum [25]. As follows from Fig.3, the increase in temperature results in the shrinkage of domains in the truth table. Different domains are differently sensitive to the temperature: the domains where the value of the projection of electron spin at  $T = 0$  is the result of interplay between stabilizing external field and "counteraction" of antiparallel spin alignment on the input dots are more sensitive to the increase in temperature.

In order to describe the temperature effect on the operation of the NOT-AND gate more comprehensively, we plotted in Fig.4 the dependence of modulus of  $\langle \hat{S}_{zi} \rangle$  on the output dot for the four characteristic points (see Fig.2) in the physical truth table at various values of  $H_z$ . Actually, we present data for three points only, since points "2" and "4" are absolutely equivalent. Although our choice is rather arbitrary, it is conditioned by the demand for the symmetry of  $H_A; H_B$  values. Besides,  $H_A = t; H_B = t$  should not be very large. Solid line corresponds to the point "1", dashed line stands for the point "2", long dashed line for "3".

Let us introduce the critical temperature  $T_c$  as a maximal temperature at which the logical function of the NOT-AND gate can be implemented (at fixed values of  $H_A; H_B$  and  $H_z$ ). The procedure to determine  $T_c$  is as follows (see Fig.4b for the sake of definiteness). Having fixed the value of  $S_t$  (in our case  $S_t = 0.5$ ), we draw a horizontal line in the plot  $\langle \hat{S}_{zi} \rangle$  vs.  $T$ . We remind that the line  $\langle \hat{S}_{zi} \rangle = 0.25$  corresponds to the value  $S_t = 0.5$ . The first intersection of the horizontal line with curves on the plot gives the value of  $T_c$ . In our case the first intersection is associated with the domain "2". Thus,  $T_c = 0.06t$  for  $H_z = 0.03t$ . Note that at the value of the external field close to the optimum one, curves standing for domains "1" and "2" practically coincide, whereas at large values of  $H_z$  the value of  $T_c$  is not governed by the domain "2" but "1".

Making use of the data presented in Fig.4 we can plot for the NOT-AND gate the phase diagram "critical temperature vs. stabilizing external field", see Fig.5. The region "1" corresponds to the parameter range at which the NOT-AND gate works. The operation of the gate is not possible for the region "2". As follows from Fig.5, if the value of  $H_z$  is small enough, the operation of the NOT-AND gate at finite temperatures may be stabilized by the increase in  $H_z$ . But if  $H_z$  is close to its optimum value the temperature enhancement results in the break down of the operation of this gate.

As follows from Figs.4,5, to provide the operation of the NOT-AND gate, the inequality  $T < H_z \mu$  must be fulfilled. But in reality more stringent condition

$$T \ll H_z \mu \quad (3)$$

must be met in order to decrease the probability to read out the erroneous result of calculations ( $S_t$  must be close to unity;  $S_t = 0.5$  gives the correct result to a probability of 75 per cent only).

Let us estimate the value of  $T$ . Taking into account the theoretical estimations [32] of the Coulomb repulsion between electrons on a quantum dot  $U \approx 10^2$  eV (that is in agreement with the experimental data [23], and the condition for strong antiferromagnetic correlations in the system  $t \ll U$  we obtain  $t \approx 10^3$  eV. Thus, for the realistic values of magnetic field  $H_z \approx 10^2$  to  $10^5$  eV  $\approx 1$  T the condition (3) gives  $T \approx 0.01$  to  $0.1$  K. Although such low temperatures may be reached in experiment, it is much lower than even the temperature of liquid helium, so the practical implementation of computations on the basis of quantum-dot spin gates seems to be hardly possible. Thus, even the fundamental limitations inherent for quantum-dot gates (such as low operation speed) or for the ground state calculation concept itself (the possibility for the system to be trapped in a local minimum giving rise to the erroneous result of calculation) would be circumvented, the effect of finite temperatures is very serious obstacle for the ground state calculations in quantum-dot spin gates.

Notice, that the approach based on non-dissipative dynamics of interacting electrons in tunnel-coupled quantum dots [27], [28] may be used for implementation of various logical functions in quantum dot spin gates in an extremely short time for realistic magnetic fields. Though for the non-dissipative computing concept there remain problems to be solved (e.g. how to prepare the system in the predetermined initial state, and to read out the result of calculation) this approach appears to be perspective for quantum dot systems.

To conclude, we have studied the effect of temperature on the operation of the elementary quantum-dot spin gates for single-electron computing within the framework of the Hubbard model by the example of the NOT-AND gate. The calculated values of the uniform external magnetic field necessary to realize the whole truth table proved to be unreasonably high for the practical implementation of the NOT-AND logical function even at the liquid helium temperature. Though in the present paper we list results for the NOT-AND gate only, for other logical gates investigated by us (e.g. AND, OR, NOR, NXOR) the critical temperature is the same to the order of magnitude [33]. Thus, this result appears to be common to all spin gates, so finite temperatures seem to be a serious obstacle for the ground state calculation concept in quantum dot spin gates.

#### Acknowledgments

This work was supported in part by the Russian Foundation for Fundamental Research under Grant No 96-02-18918 and by the Russian State Program "Advanced Technologies and Devices in Micro- and Nanoelectronics" under Grant No 02.04.329.89.5.3, and State Program "Integratsia". We would like to thank L A Openov, S N M obtkov, and S S Nazin for fruitful discussions.

- 
- [1] Gordon Moore, one of the founders of the Intel Corporation observed in the 1960s that the characteristic size for a device on a semiconductor chip was decreasing by a factor of 2 every 18 months. This empirical trend has continued up to now.
  - [2] H Luth, Phys. Stat. Sol., (b)192 (1995) 287.
  - [3] Michael S Montemero et al., Technologies and Designs for Electronic Nanocomputers. <http://www.mit.edu/research/nanotech>
  - [4] Special Issue on Quantum Information, Physics World, (March 1998) 33.
  - [5] R Feynman, Intern. J. Theor. Phys., 21 (1982) 467.
  - [6] D Deutsch, Proc. Roy. Soc. Lond., A 400 (1985) 96.
  - [7] C H Bennett, Physics Today (October 1995) 24, and references therein.
  - [8] M Plenio, V Vedral and P Knight, Physics World, (October 1996) 19.
  - [9] P Shor, Proc. of the 35th Annual Symposium on the Foundations of Computer Science, IEEE Computer Society Press, Los Alamitos, CA, (1994) 124.
  - [10] There exists another example of an algorithm that works faster on quantum computer, than on its classical counterpart { the problem of efficient search in a database. L Grover, Proc. of the 28th Annual ACM Symposium on Theory of Computing, (1996) 212.
  - [11] Q A Turchette, C J Hood, W Lange, H Mabuchi, and H J Kimble, Phys. Rev. Lett., 75 (1995) 4710.

- [12] C Monroe, D M Meekhof, B E King, W M Itano, and D J Wineland, *Phys. Rev. Lett.*, 75 (1995) 4714.
- [13] R Landauer, *Trans. Royal Soc. London, Ser. A* 353 (1995) 367.
- [14] R Landauer, *Phys. Lett.*, A 217 (1996) 188.
- [15] C Monroe, D Wineland, *Physics Today* (November 1996) 108.
- [16] K E Drexler, *Engines of Creation*, Anchor Press, Doubleday, Garden City, New York, 1986.
- [17] L Adleman, *Science* 266 (1994) 1021.
- [18] R J Lipton, *Science* 268 (1995) 542.
- [19] C S Lent, and P D Tougaw, *J. Appl. Phys.*, 74 (1993) 6227; C S Lent, P D Tougaw, W Porod, and G H Bernstein, *Nanotechnology*, 4 (1993) 49.
- [20] A N Korotkov, *Appl. Phys. Lett.*, 67 (1995) 2412; A N Korotkov, R H Chen, K K Likharev, *J. Appl. Phys.*, 78 (1995) 2520.
- [21] S Bandyopadhyay, B Das, and A E Miller, *Nanotechnology*, 5 (1994) 113; S Bandyopadhyay, V P Roychowdhury, and X Wang, *Phys. Low-Dim. Struct.*, 8/9 (1995) 28.
- [22] J S Hall, *Nanotechnology*, 5 (1994) 157.
- [23] B Meurer, D Heitmann, and K Ploog, *Phys. Rev. Lett.*, 68 (1992) 1371.
- [24] S N Moltkov, and S S Nazin, *Pis'ma v ZhETF*, 62 (1995) 256 [*JETP Lett.* 62 (1995) 273]; *ZhETF* 110 (1996) 1439 [*JETP* 83 (1996) 794].
- [25] A V Krasneninnikov, and L A Openov, *Pis'ma v ZhETF*, 64 (1996) 214 [*JETP Lett.* 64 (1996) 231].
- [26] S N Moltkov, and S S Nazin, *Phys. Low-Dim. Struct.*, 10 (1997) 85.
- [27] A M Bychkov, L A Openov, and I A Semihin, *Pis'ma v ZhETF*, 66 (1997) 275 [*JETP Lett.* 66 (1997) 298].
- [28] L A Openov and A M Bychkov, *Phys. Low-Dim. Struct.*, 9/10 (1998) 153.
- [29] K Nomoto, R Uga, T Suzuki, and I Hase, *J. Appl. Phys.*, 79 (1996) 291.
- [30] J Hubbard, *Proc. Roy. Soc., A* 276 (1963) 238.
- [31] V F Elesin, A V Krasneninnikov, and L A Openov, *Zh. Eksp. Teor. Fiz.*, 106 (1994) 1459; *ibid* 107 (1995) 2092 [*JETP* 79 (1994) 789; *JETP* 80 (1995) 1158]; *Phys. Rev. B* 52 (1995) 16187.
- [32] A V Krasneninnikov, S N Moltkov, S S Nazin, and L A Openov, *ZhETF*, 112 (1997) 1257 [*JETP* 85 (1997) 682].
- [33] A V Krasneninnikov, R A Koltsov, unpublished.

# FIGURE CAPTIONS

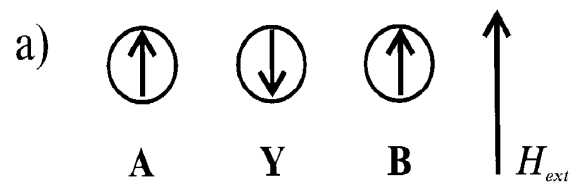
Fig.1. Three-dot NOT-AND gate. (a) Physical implementation; (b) Logical truth table.

Fig.2. Physical truth table of the NOT-AND gate.  $U=t=20$ ;  $H_z=t=0.01$ ,  $S_t=0.95$ ,  $T=0$ . The four characteristic points (see text) are indicated.

Fig.3. Physical truth tables of the NOT-AND gate at various temperatures.  $U=t=20$ ;  $H_z=t=0.05$ ,  $S_t=0.5$ . a)  $T=t=0$ ; b)  $T=t=0.08$ ; c)  $T=t=0.085$ ; d)  $T=t=0.095$ .

Fig.4. Temperature dependence of modulus of  $\hat{h}_z^i$  on the output dot for the characteristic points (see Fig.2) in the physical truth table at various values of  $H_z$ . Solid line corresponds to the point \1", dashed line stands for the point \2", long dashed line for \3". a)  $H_z=t=0.01$ ; b)  $H_z=t=0.03$ ; c)  $H_z=t=0.05$ ; d)  $H_z=t=0.07$ .

Fig.5. The phase diagram \critical temperature  $T$  vs. stabilizing external magnetic field  $H_z$ " for the NOT-AND gate. The region \1" corresponds to the parameter range at which the NOT-AND gate works. The operation of the gate is not possible for the region \2".

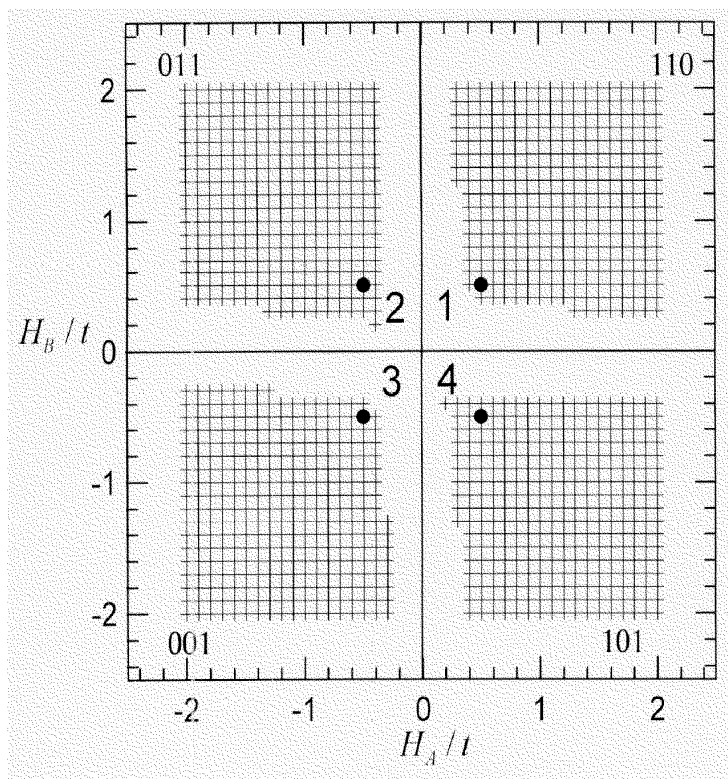


b)

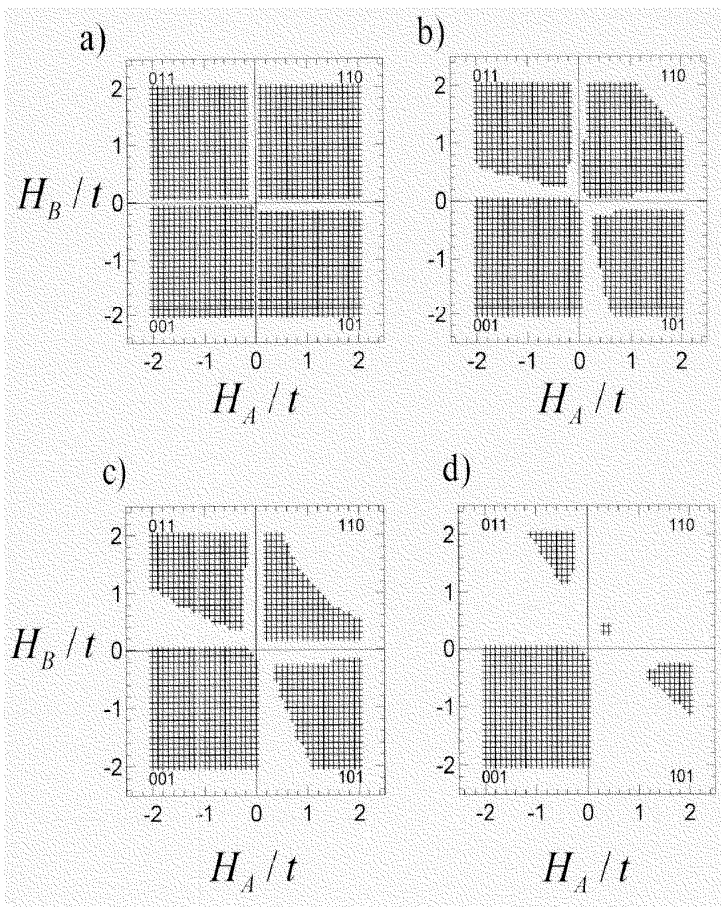
A	B	Y
1	1	0
0	1	1
1	0	1
0	0	1





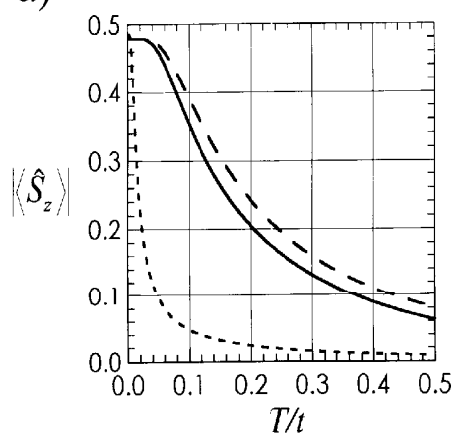




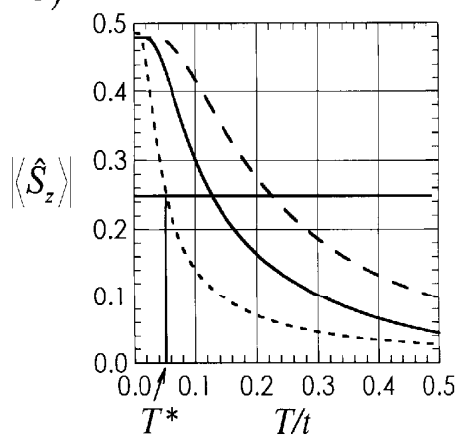




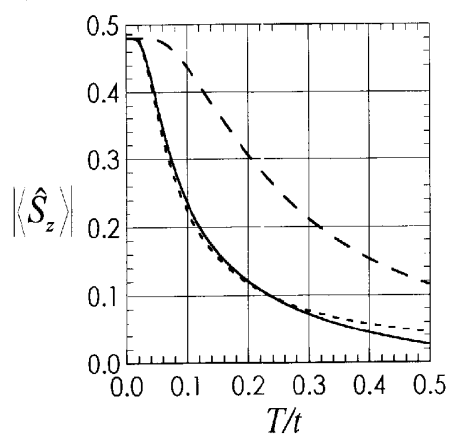
a)



b)



c)



d)

